GPS Satellite Signal Strength Model for Ionospheric Total Electron Content in Sarawak, Malaysia

Voon Pai Bong, Wan Azlan Wan Zainnal Abidin, Mardina Abdullah, Kismet Hong Ping, Thelaha Masri, Shapiee Abdul Rahman, Siti Aminah Bahari, Ibrahim Abba

Abstract— Satellite signals for communication and navigation experience impairment effects due to ionosphere especially in the equatorial region. The causes and significance of ionosphere disturbances are a kind of research that is of great interest in this area. Space-based radio communication systems such as the Global Positioning System (GPS) is providing a unique chance to explore the impact of the ionosphere as the signals propagate from the satellites to the GPS receivers. Sarawak which is located near to the equatorial region has been selected for the aim of this research. By utilizing the Total Electron Content (TEC), data recorded by the GPS Ionospheric Scintillation & TEC Monitor (GISTM), the ionospheric effect was examined and related to the signal strength performance. The recorded TEC were tested by comparing to TEC obtained from CODE Global Ionosphere Maps (GIMs) in time series. The results have shown a high consistency of TEC in the time domain with their corresponding minimum and maximum values of TEC that occurred at the same time. The preliminary developed SNR empirical model using regression curve fitting approach is a function of slant TEC from the satellites to the reference station path. This model will be used to forecast the satellite signal strength performance with an input parameter of slant TEC.

Index Terms— Global Positioning System, Total Electron Content, ionosphere, signal-to-noise ratio, empirical model.

1 INTRODUCTION

INCREASING demand for a better modeling and understanding of the behavior of the satellite signal strength is required by the scientific community. The satellite signal strength is measured from Global Positioning System (GPS) satellites to ground receiver. The GPS satellite signal strength performance is studied based on a parameter of signal-to-noise ratio (SNR) in a 1 Hz-bandwidth [1], where larger SNR indicates a stronger signal. It is a function of transmitted signal, distance and receiver hardware with a value which is typically 30 to 55 dBHz at outdoors [2].

GPS is a space-based radio navigation system operated and maintained by the United States Air Force for the United States Department of Defense [3]. It has become increasingly sophisticated and widespread and started to be integrated into the user's mobile terminal units [4]. It is a system made up of a network of twenty-four satellites, which are shared in six orbital planes around the space at an altitude of about 20,200 km [5].

Besides, a research study of the ionosphere is getting much interest recently. The ionosphere represents the largest source of GPS signal error since the selective availability was turned off in May 2000 [6]. Consequently, one of the coming challenges of the space weather community is to predict the satellite signal strength performance in response to variations in ionospheric activity. In Malaysia, a few research works on equatorial ionosphere have been done [7], [8], [9], [10]. The presence of the equatorial anomaly in Malaysia has been confirmed based on the Total Electron Content (TEC) performance at ionosphere [7]. There are diurnal and seasonal variation of ionospheric activity at the equatorial station are presented and discussed [8]. The highest values for TEC are obtained around post noon while the minimum TEC occur in the post-midnight. In the seasonal variation, the highest TEC is found in equinoctial months and the lowest TEC is found in summer. Moreover, solar eclipse affects the ionospheric layer which can cause the ionospheric disturbance in Malaysia has been reported [9]. Furthermore, ionospheric scintillation and TEC fluctuation was investigated at Universiti Kebangsaan Malaysia station, Malaysia between September 2009 and December 2010 [10]. The study shows that night time amplitude scintillation always occurred with phase scintillation, TEC depletions, rate of change of TEC (ROT) fluctuations and the enhancement of the rate of TEC index. Nevertheless, during the daytime, amplitude scintillation, TEC depletions and ROT fluctuations were much weaker than those that occurred during night time.

The parameter of the ionosphere that provides most of the effects on GPS signals is known as TEC [11], [12]. TEC is the measure of the total number of free electrons in a column of

- *Voon Pai Bong is currently pursuing doctoral degree program in Electrical and Electronic Engineering in Universiti Malaysia Sarawak, Malaysia. E-mail:13010149@siswa.unimas.my*
- *Wan Azlan Wan Zainal Abidin is a senior lecturer of Department of Electrical and Electronic Engineering, Universiti Malaysia Sarawak, Malaysia. E-mail: wzaazlan@feng.unimas.my*
- *Mardina Abdullah is a head of Space Science Center: ANGKASA, Universiti Kebangsaan Malaysia. Email: mardina@ukm.edu.my*
- *Kismet Hong Ping is a senior lecturer of Department of Electrical and Electronic Engineering, Universiti Malaysia Sarawak, Malaysia. Email: hpkismet@feng.unimas.my*
- *Shapiee Abdul Rahman is senior lecturer of Department of Computational Science and Mathematics, Universiti Malaysia Sarawak, Malaysia. Email: sar@fit.unimas.my*
- *Siti Aminah Bahari is currently pursuing doctoral degree program in Electrical, Electronic and System Engineering, Universiti Kebangsaan Malaysia. Email: sitiaminahbahari@ukm.edu.my*
- *Ibrahim Abba is currently pursuing doctoral degree program in Electrical and Electronic Engineering, Universiti Malaysia Sarawak, Malaysia. E-mail:120100130@siswa.unimas.my*

the unit cross section along the path of the electromagnetic wave between the ground receiver and the GPS satellite. Therefore, it is an indicator of ionospheric variability derived from the modified GPS signal through free electrons. TEC is measured in TEC unit (TECU) of 10^{16} electrons per meter squared. The nominal limit is 10^{16} to 10^{19} with its minimum and maximum occurring at midnight and mid-afternoon approximately. At night, the TEC decays very slowly due to recombination of electrons and ions [13]. In fact, the number of free electrons is driven by the ionization and recombination processes of the ionosphere, and these processes are in turn driven mainly by extreme ultraviolet radiation from the sun [14]. There is also a geographic variability in the electron content with the highest electron density in the equatorial region and the lowest density in the mid-latitude regions [15].

In a global scale, global ionosphere maps (GIMs) are used as a reference. GIMs are generated on a daily basis at Center of Orbit Determination in Europe (CODE) using data from about 200 GPS sites of the International GPS Service (IGS) and other institutions [16]. GIMs indicate TEC data measured by the GPS stations and these two L-band frequencies are called as L1 (1575.42 MHz) and L2 (1227.60 MHz) [17]. All the analysis centers involved may use different approaches to the TEC derivation from GPS observations, as well as different TEC representation or modeling techniques. The spatial resolution of the final CODE GIMs is 2.5^{o} in latitude and 5.0^{o} in longitude as well as 2 hours temporal resolution. In the GIMs, it is assumed that the ionosphere is concentrated in a thin shell at 450 km altitude and the grid points are fixed in a solar geomagnetic coordinate system. Besides, TEC GIMs have a standard deviation ranging from 0.7 to 6.0 TECU and an announced accuracy of the order of 2 to 8 TECU [18]. Consequently, GIMs are a good indicator of the ionospheric activity and give the opportunity to study and verify the global climatological behavior of the TEC over a complete solar cycle.

The present paper aims at establishing the basis to model the variation behaviors of the SNR with respect to slant TEC which best suits in Sarawak region. In this paper, strategies to determine the TEC and development of the signal strength empirical model in Sarawak region using the GPS Ionospheric Scintillation and TEC Monitor (GISTM) data are described in Section 2. In Section 2.1, the data collection and acquisition are described. Then, calculation of vertical TEC by using mapping function is described in Section 2.2. Section 2.3 is discussed the development of signal strength's empirical model. Methodology of TEC calculation from CODE GIMs is explained in Section 2.4 for TEC verification used. The results and discussion of the climatological model of satellite signal strength are dedicated in Section 3 as well as the verification test of the model. Finally, Section 4 gives the conclusions.

2 METHODOLOGY

The methodology of this project contains two categories that are data collection and acquisition as well as data analyzing method. Data collection and acquisition contains the description about the GPS data that has been used. Then, data analyzing method categories is describing how the data will be processed, then to be analyzed, modeled and verified. The research methodology is shown in Fig. 1. Raw data are measured and obtained from UNIMAS station. Then, the data will be processed in order to extract the required parameters for further analysis. The measured TEC from GISTM can be verified by comparing with TEC obtained from CODE GIMs in time series. After that, SNR is modeled in terms of slant TEC based on the measured data. The formulated model will be verified by comparing with actual data. The detail of the methodology will be further explained in the next section.

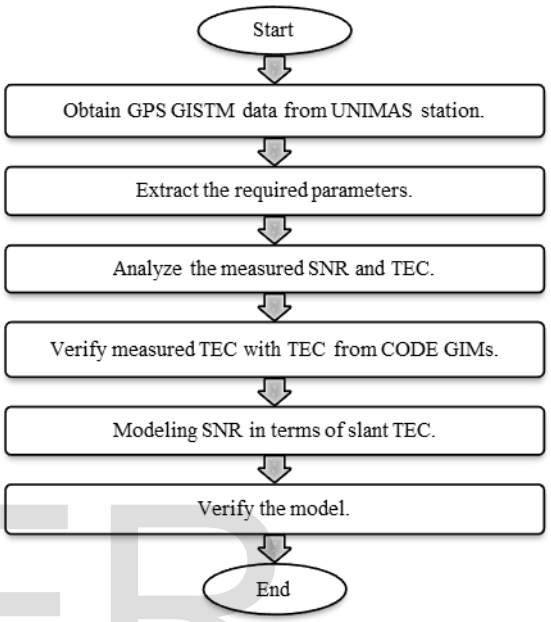

Fig. 1. Flowchart of the research.

2.1 Data Collection and Acquisition

Data collection is carried out by using GISTM receiver under clear sky environment. Under collaboration work with the Space Science Centre - (ANGKASA), Universiti Kebangsaan Malaysia (UKM), the GISTM receiver was placed on the rooftop of Faculty of Engineering building at Universiti Malaysia Sarawak (UNIMAS). This receiver comprises the major component of the GPS signal monitor, specifically configured to measure amplitude and phase scintillation from the L1 frequency GPS signals, and ionospheric TEC from the L1 and L2 frequencies GPS signals. This scintillation and TEC monitoring receiver is a low phase noise oscillator and provides true amplitude, single frequency carrier phase measurements and TEC measurements from up to 11 GPS satellites in view. A month of raw data with daily 24 hours observation in 60 second's interval is used and processed to extract the parameters for those visible GPS satellites.

The required parameters such as GPS time of week (GPS TOW), pseudorandom number (PRN) of the visible satellite, elevation angle, SNR and TEC values are extracted. The extracted data file is then being programmed to separate the required data based on satellites. Further programming is done to analyze and model the received satellite signal strength performance in terms of slant TEC.

2.2 Vertical Total Electron Content Calculation using Mapping Function

TEC (also named as slant TEC) measurements are taken from different GPS satellites observed at arbitrary elevation angles. This causes the GPS signals to cross large different portion of the ionosphere. To compare the electron contents for paths with different elevation angles, the slant TEC (sTEC) must be transformed into equivalent vertical content or vertical TEC (vTEC) by using a suitable mapping function. As sTEC is a quantity that is dependent on the ray path geometry through the ionosphere, it is desirable to calculate an equivalent vertical value of TEC that is independent of the elevation of the ray path [19].

The single-layer (or thin-shell) model was employed to determine the absolute vTEC [20]. Single-layer model (SLM) assumes that all the free electrons contain in a shell of infinitesimal thickness at an altitude of about 450 km above the earth's surface. The point where the vTEC is determined is called the Ionospheric Pierce Point (IPP). It is the intersection of the receiver line-of-sight to the tracked satellite with the center of the ionospheric slab as shown in Fig. 2.

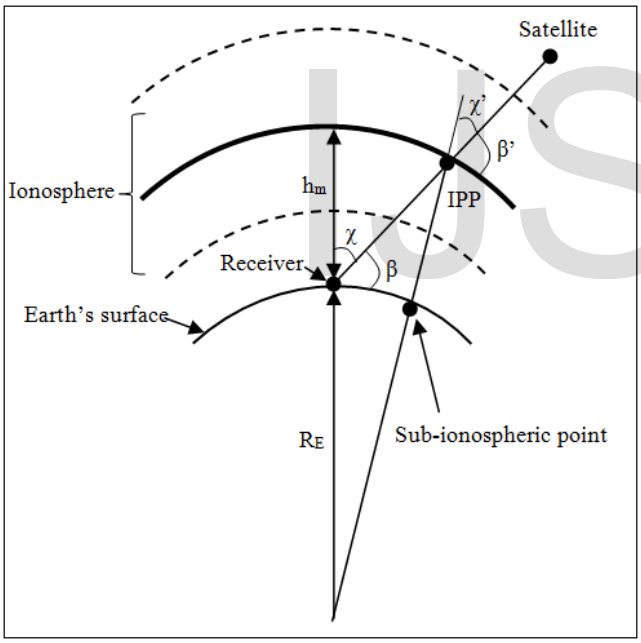

Fig. 2. Single-layer model for the ionosphere.

By referring to Fig. 2, vTEC through a given sub-ionospheric point is obtained as shown in (1).

$$vTEC = sTEC(\cos\chi'). \quad (1)$$

The SLM mapping function can be written as in (2) which describe the ratio between the sTEC and vTEC.

$$F(\chi) = \frac{TEC(\chi)}{TEC(0)} = \frac{1}{\cos\chi' or \sin\beta'} = \frac{1}{\sqrt{1-\sin^2\chi'}} \quad (2)$$

with

$$\sin\chi' = \frac{R_E}{R_E + h_m}\sin\chi \quad (3)$$

$$\chi' = \sin^{-1}\left(\frac{R_E}{R_E + h_m}\sin\chi\right) \quad (4)$$

$$\chi' = \arcsin\left(\frac{R_E}{R_E + h_m}\sin\left(\frac{\pi}{2} - \beta\right)\right) \quad (5)$$

where χ and χ' are the zenith angles at their receiver site and at the IPP, respectively, β and β' are the elevation angles at the receiver site and at the IPP, respectively, R_E is the mean earth radius and h_m refers to the height of maximum electron density. Hence, vTEC is written as in (6).

$$vTEC = sTEC \times \cos\left\{\arcsin\left[\frac{R_E \sin\left(\frac{\pi}{2} - \beta\right)}{R_E + h_m}\right]\right\} \quad (6)$$

A typical value for R_E and h_m are set to 6371 km and 450 km, respectively [19]. The more precise mapping function according to [21] and currently applied in the IGS Global TEC map is the modified single layer model, M-SLM that is defined as in (7),

$$\sin\chi' = \frac{R_E}{R_E + h_m}\sin(\alpha\chi) \quad (7)$$

where α is a correction factor which is close to unity.

2.3 Development of Signal Strength's Empirical Model

Empirical modeling involves examining data related to the problem with a view of formulating or constructing a mathematical relationship between the variables in the problem using the available data [22]. In this research, the signal strength empirical model is developed from the measurement results obtained under the open space condition. The purpose of this empirical model is to study and forecast the signal strength performance in terms of ionospheric effect. The model will be derived mathematically from the relationship of the average SNR with slant TEC from those visible satellites in the open space environment. The model is developed by using the regression curve fitting approach [23]. Curve fitting is the process of constructing a curve or findings mathematical function to approximate straight lines or curves that best fit given sets of data. Linear, parabolic regression and regression with power series approximations will be applied. Those regressions are performed with the method of least squares. Lastly, the best fitting curve is chosen. SNR also can be modeled in terms of vTEC and elevation angle by using the mathematical relationship in (6).

2.4 TEC Calculation from CODE GIMs

The IONosphere map Exchange (IONEX) file is downloaded from CODE [16]. The calculation of TEC from the IONEX file is done by first choosing the nearest latitude in the file with the latitude of the location. The latitude and longitude of the chosen location are 1.483°N and 110.333°E, respectively. The nearest latitude to 1.483°N in the IONEX file is 2.5°N. The longitude in the file is between -180°E to 180°E by an increment of 5°. Hence, the longitude of 110°E and 115°E which are closer to the longitude of 110.333°E will be referred. Table 1 shows a sample of TEC values on the latitude of 2.5°N and longitude

from -180°E to 180°E with increment by 5.0° consecutively. The recorded data is referred to a 450 km ionospheric height from the Earth's surface at 8:00 am on 5 September 2014.

TABLE 1
A sample of TEC values on LAT/LON1/LON2/DLON/H of 2.5°N, -180°E, 180°E, 5.0° and 450 km at 8:00 am on 5 September 2014.

2.5	-180.0	180.0	5.0	450.0							LAT/LON1/LON2/DLON/H					
626	631	653	677	690	692	693	698	706	715	727	743	746	723	677	629	
598	579	554	514	467	419	372	321	271	230	199	169	142	134	164	224	
281	303	286	252	223	205	190	175	165	160	154	143	128	114	102	91	
81	73	68	64	65	79	112	157	199	230	253	277	307	342	381	427	
474	512	537	558	583	612	631	632	626								

The TEC values unit given in the IONEX file is 0.1 TECU. The circle in Table 1 shows the value of 253 and 277 which are corresponding to TEC values at the longitude of 110°E and 115°E, respectively. From these two values, TEC values at the longitude of 110.333°E can be calculated by applying interpolation technique. Therefore, on 5 September 2014 at 8:00 am, the place with latitude and longitude of 1.483°N and 110.333°E respectively has estimated TEC values of 25.4 TECU. These processes are continuously calculated for every two hours for a 24-hour data.

3 Results and Discussion

In order to study the satellite signal strength performance, a set of GPS sample data for September 2014 from UNIMAS, Kota Samarahan, Sarawak (1.28°N, 110.26°E) was collected, processed and analyzed. The GPS data was recorded daily in the universal time system, with the sampling interval of 60 seconds and analyzed with cut-off elevation mask of 15°.

In this section, the relationship between SNR and slant TEC for the clear sky environment are investigated, analyzed and presented in graphical forms. Then, a fundamental empirical model is developed and verified.

The sTEC and vTEC values were obtained according to the methodology presented by using programming software. Both sTEC and vTEC against local time for all of the visible satellites are shown in Fig. 3 and Fig. 4, respectively. Local time (LT) is obtained by adding 8 hours to the corresponding universal time. Daytime variation in TEC shows large variability in comparison to night time variation. During night time, the TEC decays because of recombination of electrons and ions. However, during the daytime, the sun emits particles in the ionosphere thus increasing the density of electrons. This diurnal variation occurs because of the daily rotation of the Earth on its axis, following the apparent movement of the Sun [24]. In both of these figures, TEC exhibits the typical characteristics with other equatorial and low latitude ionosphere [11], [25].

In order to compare the electron contents for paths with different elevation angles, the sTEC has been transformed into equivalent vTEC as mentioned in the methodology. STEC has values in the range from 0 TECU to 145 TECU as shown in Fig. 3, while vTEC has values in the range from 0 TECU to 66 TECU as shown in Fig. 4. Therefore, it is clear that the vTEC shows lower readings as compared to its corresponding sTEC which similar with previous research findings by Bagiya et al. [11], Bolaji et al. [25] and Leong et al. [26].

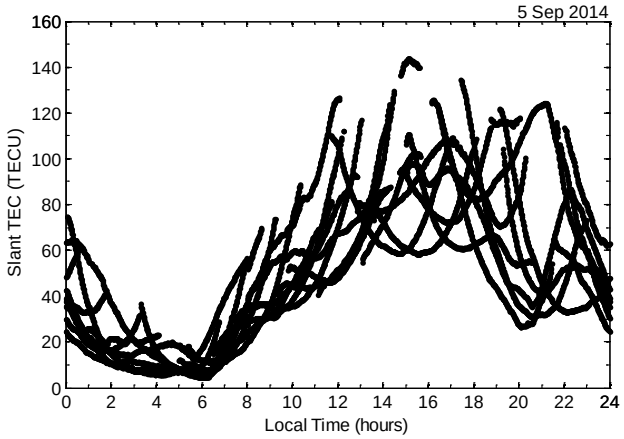

Fig. 3. Slant TEC against local time for the visible satellites.

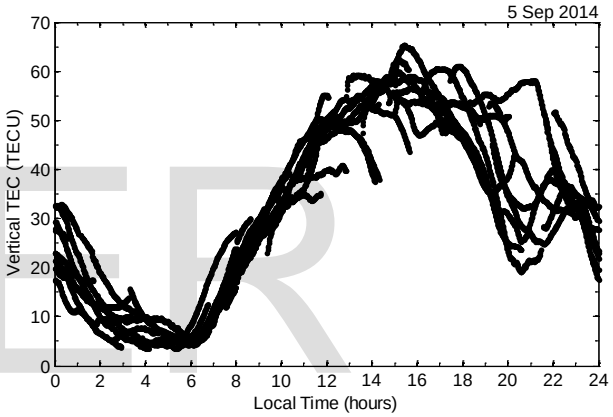

Fig. 4. Vertical TEC against local time for the visible satellites.

The smoothed sTEC and vTEC against local time based on daily data in September 2014 are plotted as shown in Fig. 5. These curves are obtained by applying one hour moving average method on the daily data. A moving average method smoothed the data by plotting points that are the average of several time intervals [27]. Then, the average of daily smoothed TECs against local time is taken. This result's curve would be much smoother than actual data's curves. Furthermore, the results in Fig. 5 show the peak of sTEC and vTEC points at 17-LT and 14-LT respectively as well as the lowest at 6-LT. Therefore, the maximum TEC occurs in the post local noon, and minimum TEC occurs just before sunrise are observed which agrees with finding by Jensen and Mitchell [28]. The vTEC have also shown a smooth rising trend starting from 6-LT to 14-LT which is similar with finding by Bagiya et al. [11].

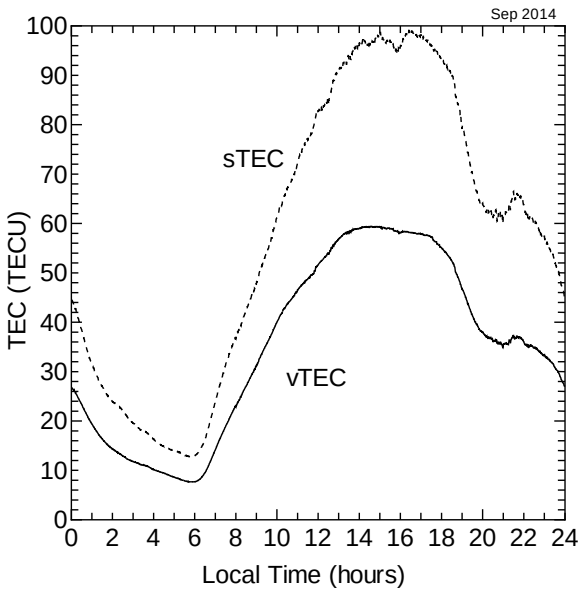

Fig. 5. Smoothed sTEC and vTEC against local time.

In order to validate the measured vTEC from GISTM, a comparison to vTEC from CODE GIMs was performed. The vTEC results in time domain from GISTM and CODE GIMs were shown in Fig. 6. In general, the measured vTEC is comparable to the vTEC from CODE GIMs. It is noticeable that GIMs' vTEC level is higher in the range of 0.5 to 18 TECU as compared to the measured vTEC from GISTM. The difference in scale factor between these curves are because there was no IGS station placed in Malaysia [29]. As mentioned in the introduction, IGS GIMs are a combination of GIMs provided by several analysis centers. Therefore, the vTEC are estimated from CODE GIMs via an interpolation method. However, the diurnal characteristic of ionospheric variation from both curves showed a good agreement. This result has shown high consistency of vTEC in time domain with their corresponding minimum and maximum values of vTEC that occurred at the same time.

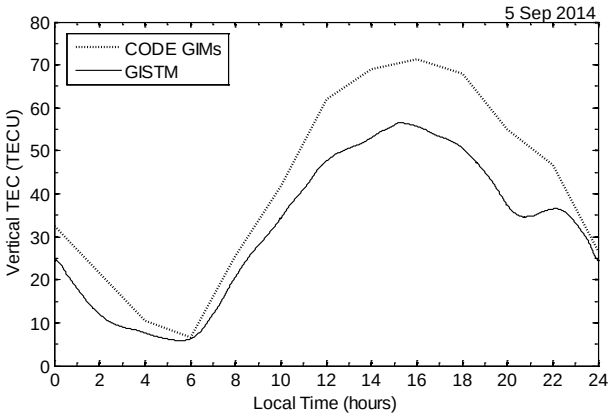

Fig. 6. Comparison of vTEC from CODE GIMs and GISTM.

Furthermore, Fig. 7 shows the plot of average SNR against sTEC by using raw data collected from GISTM for September 2014. All of the visible satellite signal's data are included in the computation of Fig. 7. The regression curve fitting approach is applied to model the measured data as shown in Fig. 8.

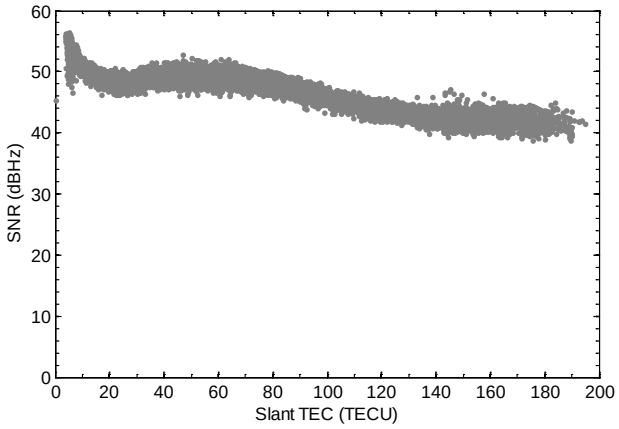

Fig. 7. Average SNR against sTEC for September 2014.

Regression calculates an equation that minimizes the distances between the fitted curve and all of the data points [30]. In general, a model fits the data well if the difference between the observed values and the model's predicted values are small and unbiased. For analysis purpose, residual plots can reveal unwanted residual patterns that indicate biased results more effectively than numbers [31]. When the residual plots pass muster, the numerical results can be trusted and the goodness-of-fit statistics could be checked. R-squared is a statistical measure of how close the data are to the fitted regression curve [32]. R-squared is always between 0% and 100%. 0% indicates that the model explains none of the variability of the response data around its mean, while 100% indicates that the model explains all the variability of the response data around its mean. In general, the higher the R-squared, the better the model fits the data.

Fig. 8(a) shows the linear regression with the R-squared value equal to 0.8297 where there is 82.97% of the data can be calculated from the linear regression equation. However, Fig. 8(b) shows the exponential regression where it has lower R-squared value of 0.8238 as compared to linear regression. Fig. 8(c) and Fig. 8(d) show the logarithmic and power regression curves where they have lower R-squared value of 0.6646 and 0.6465 respectively. Besides, quadratic polynomial regression curve with higher R-squared value of 0.8391 is shown in Fig. 8(e). The least-squares regression curve with highest R-squared value among the others is shown in Fig. 8(f). As a result, this cubic polynomial regression is used to fit the data in order to model the relationship of SNR in terms of sTEC. This regression gives R-squared value of 0.8559 where 85.59% of the variance in the SNR values can be accounted for by this cubic polynomial regression equation. The corresponding mathematical equation of SNR in terms of sTEC is shown in (8).

$$SNR = (3.997\times10^{-6})sTEC^3 - 0.0012sTEC^2 + 0.0441sTEC + 49.533 \quad (8)$$

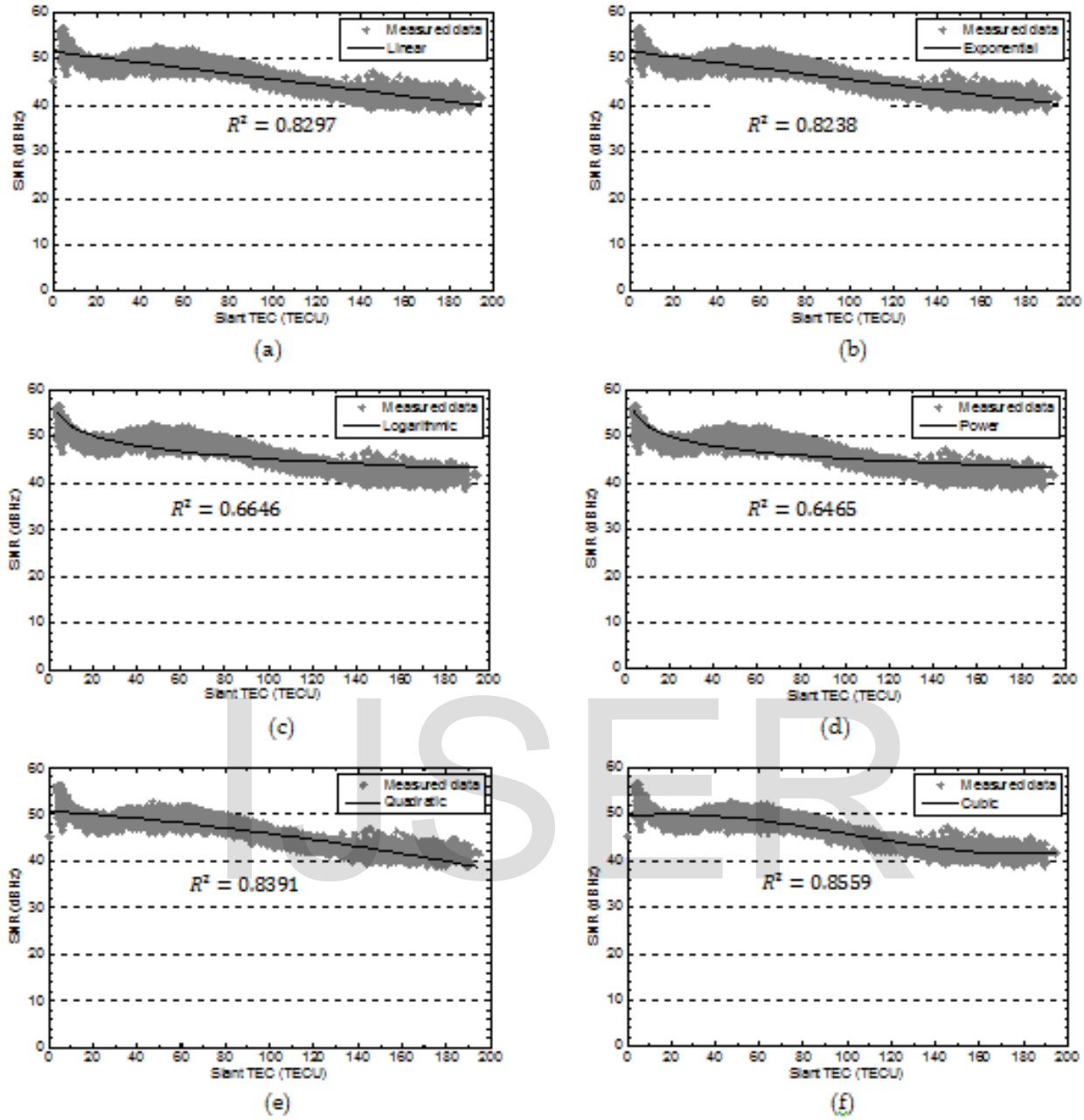

Fig. 8. Regression curve fitting for measured average SNR against sTEC. a) Linear regression fitting of the measured data. b) Exponential regression fitting of the measured data. c) Logarithmic regression fitting of the measured data. d) Power regression fitting of the measured data. e) Quadratic regression fitting of the measured data. f) Cubic regression fitting of the measured data.

The trend of SNR at certain sTEC can be estimated and studied by using this mathematical equation. Therefore, the received signal strength can be predicted if sTEC is known. In addition, sTEC in terms of vTEC and elevation angle, β as given in (9) is formulated from methodology presented. Here, a correction factor is assumed to be equal to unity. By substituting (9) into (8), SNR in terms of vTEC and β can be formulated. Thus, the received signal strength can also be estimated and studied if vTEC and β are known.

$$sTEC = \frac{vTEC}{\cos\left[\arcsin\left(0.934\cos\beta\right)\right]} \tag{9}$$

The residual which is the difference between the measured value and predicted value is used to obtain residual plot as shown in the bottom plot of Fig. 9. The points in residual plot are randomly dispersed around the horizontal axis which satisfies that the cubic regression model is appropriate for the data. However, there are significant variations in SNR at smaller sTEC values, since there are larger residuals occurred at smaller sTEC values compared with the higher sTEC values. Moreover, it can be observed that the SNR value gradually decreases when the sTEC is increases as shown in the upper plot of Fig. 9. These results are similar with finding by Das-

Gupta et al. [33], where the satellite signal strength decreases when the ionospheric effect increases.

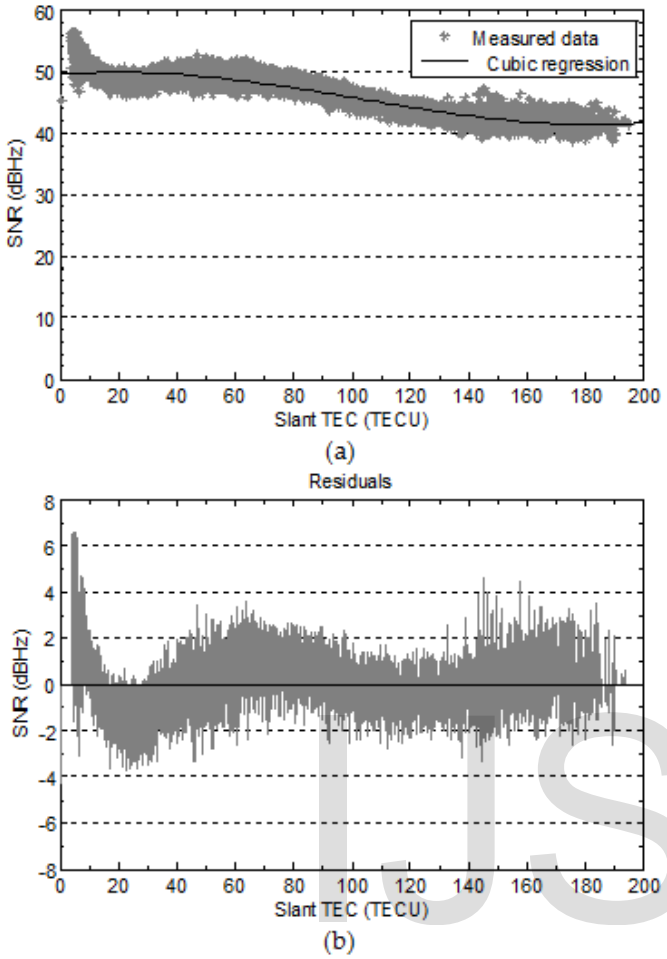

Fig. 9. Measured data and cubic polynomial best fit regression as well as its residual plot.

In order to verify the fitted model, measured data of satellite PRN 6 on 5 September 2014 is compared to the predicted data calculated from the model as shown in Fig. 10. Covariance describes how two variables are related. A positive covariance means the variable are positively related, while a negative covariance means the variables are inversely related. The covariance between the measured and predicted data is 1.0065. Since the covariance is positive, the variables are positively related. Hence, both sets of measured and predicted data tend to show similar behavior.

Mean absolute percentage error (MAPE) is the most common measure of forecast error by expressing accuracy as a percentage of the error. MAPE is the average absolute percentage error for each time period or forecast minus actuals divided by actuals. MAPE of 0% indicates the predicted data is 100% fit the measured data, while MAPE of 100% indicates both of the predicted and measured data do not fit each other. The predicted data in Fig. 10 shows very high accuracy compared to the measured data since the corresponding MAPE is only 5.70%. Therefore, it is verified that the predicted model fits the measured data well with very high accuracy and positive behavior.

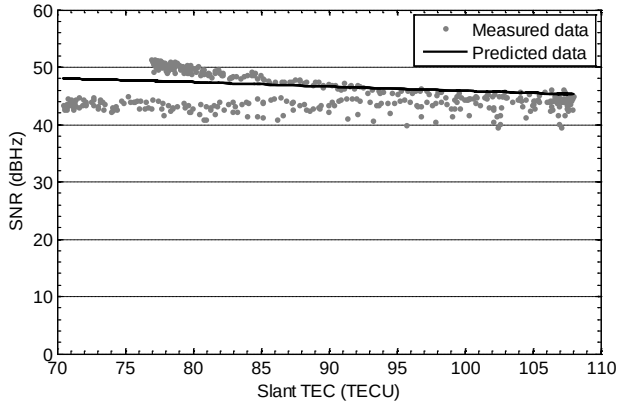

Fig. 10. Measured and predicted SNR against sTEC.

4 Conclusion

The work presented has shown encouraging results based on the utilization of TEC for the received signal strength performances. The vertical TEC had been calculated by using a single-layer model for the mapping function. The TEC data obtained from GISTM shows that the maximum TEC occurs in the post local noon, and minimum TEC occurs just before sunrise. The TEC results have been validated by comparing to the TEC obtained from CODE GIMs in the global scale. The best fit cubic polynomial regression curve as a function of sTEC have been fundamentally developed and verified based on data collected in UNIMAS, Kota Samarahan, Sarawak, Malaysia. This regression curve is forecasting the received signal strength performance in equatorial region in line-of-sight environment. This contribution will help in communication networks and navigation systems in equatorial region. In addition, a longer period of experimental data is necessary in order to characterize the satellite signal strength performance further and generate a general empirical model in this region. Furthermore, more input parameters such as elevation angle and time of a day should be considered.

Acknowledgment

The author would like to thank Universiti Malaysia Sarawak who has funded this research work. The authors also want to express grateful to Space Science Centre (ANGKASA), Universiti Kebangsaan Malaysia for providing the GISTM data.

References

[1] H.-G. Wang, Z.-S. Wu, L.-K. Lin, S.-F. Kang, and Z.-W. Zhao, "Retrieving Evaporation Duct Heights from Power of Ground-based GPS Occultation Signal," *Progress In Electromagnetics Research M*, vol. 30, pp. 183-194, 2013.

[2] C. Prakash, V.K. Chakka, S.N. Satashia, and K.S. Parikh, "Digital Receiver based Ka Band Beacon Receiver for Improved Beacon Power Estimation," in *International Conference on Communication and Signal Processing (ICCSP)*, Melmaruvathur, India, pp. 1117-1122, 2013.

[3] A. El-Rabbany, *Introduction to GPS: The Global Positioning System*, Second ed.: Artech House, Incorporated, pp. 210, 2006.

[4] F. Yang and Z. M. Wang, "A Mobile Location-based Information

Recommendation System based on GPS and WEB2.0 Service," *WSEAS Transactions on Computers,* vol. 8, pp. 725-734, 2009.

[5] E. D. Kaplan and C. J. Hegarty, *Understanding GPS: Principles and Applications*, Second ed.: Artech House, pp. 3-4, 2006.

[6] S. Dubey, R. Wahi, and A. K. Gwal, "Ionospheric Effects on GPS Positioning," *Advances in Space Research,* vol. 38, pp. 2478-2484, 2006.

[7] M. Abdullah, A. F. M. Zain, Y. H. Ho, and S. Abdullah, "TEC and Scintillation Study of Equatorial Ionosphere: A Month Campaign over Sipitang and Parit Raja Stations, Malaysia," *American Journal of Engineering and Applied Sciences,* vol. 2, pp. 44-49, 2009.

[8] Z.M. Radzi, M. Abdullah, A.M. Hasbi, J. Mandeep, and S.A. Bahari, "Seasonal Variation of Total Electron Content at Equatorial Station, Langkawi, Malaysia," in *Proceeding of the 2013 IEEE International Conference on Space Science and Communication (IconSpace)*, Melaka, Malaysia, pp. 186-189, 2013.

[9] N. Ya'acob, W.M.F.W. Hasbullah, N.F. Azmi, A.L. Yusof, and M.H. Jusoh, "GPS Ionospheric Scintillation and Total Electron Content during Partial Solar Eclipse in Malaysia," in *2014 IEEE 10th International Colloquium on Signal Processing & its Applications (CSPA2014)*, Kuala Lumpur, Malaysia, pp. 276-281, 2014.

[10] A. Seif, M. Abdullah, A.M. Hasbi, and Y. Zou, "Investigation of Ionospheric Scintillation at UKM Station, Malaysia during Low Solar Activity," *Acta Astronautica,* vol. 81, pp. 92-101, December 2012.

[11] M.S. Bagiya, H.P. Joshi, K.N. Iyer, M. Aggarwal, S. Ravindran, and B.M. Pathan, "TEC Variations during Low Solar Activity Period (2005-2007) near the Equatorial Ionospheric Anomaly Crest Region in India," *Annales Geophysicae,* vol. 27, pp. 1047-1057, 2009.

[12] U. Tancredi, A. Renga, and M. Grassi, "Validation on Flight Data of a Closed-loop Approach for GPS-based Relative Navigation of LEO Satellites," *Acta Astronautica,* vol. 86, pp. 126-135, May-June 2013.

[13] N. Ya'acob, M. Abdullah, M. Ismail, and A. Zaharim, "Model Validation for GPS Total Electron Content (TEC) using 10th Polynomial Function Technique at an Equatorial Region," *WSEAS Transactions on Computers,* vol. 8, pp. 1533-1542, September 2009.

[14] B. Zolesi and L.R. Cander, "Chapter 2 The General Structure of the Ionosphere," in *Ionospheric Prediction and Forecasting*, Springer Berlin Heidelberg, pp. 12-18, 2014.

[15] International Telecommunication Union, "Ionospheric Propagation Data and Prediction Methods Required for the Design of Satellite Services and Systems," Recommendation ITU-R P.531-12, Geneva, 2013.

[16] University of Berne, "*Global Ionosphere Maps Produced by CODE,"* aiuws.unibe.ch/ionosphere/. 2012.

[17] C.B. Erol and S.G. Tanyer, "Estimation of the Daily Mean Ionospheric Total Electron Content using Global Ionospheric Maps," in *2002 IEEE International Geoscience and Remote Sensing Symposium (IGARSS02)*, pp. 1287-1289, 2002.

[18] N. Bergeot, I. Tsagouri, C. Bruyninx, J. Legrand, J.-M. Chevalier, P. Defraigne, Q. Baire, and E. Pottiaux, "The Influence of Space Weather on Ionospheric Total Electron Content during the 23rd Solar Cycle," *Journal Space Weather Space Climate,* vol. 3, 2013.

[19] N. Ya'acob, M. Abdullah, and M. Ismail, "Leveling Process of Total Electron Content (TEC) using Malaysian Global Positioning System (GPS) Data," *American Journal of Engineering and Applied Sciences,* vol. 1, pp. 223-229, 2008.

[20] N. Ya'acob, M. Abdullah, M. Ismail, S.A. Bahari, and M.K. Ismail, "Ionospheric Mapping Function for Total Electron Content (TEC) using Global Positioning System (GPS) Data in Malaysia," in *2008 IEEE International RF and Microwave Conference Proceedings*, Kuala Lumpur, Malaysia, pp. 386-389, 2008.

[21] S. Schaer, "Mapping and Predicting the Earth's Ionosphere using the Global Positioning System," PhD dissertation, Bern University, Switzerland, 1999.

[22] B.P. Bezruchko and D.A. Smirnov, *Extracting Knowledge From Time Series An Introduction to Nonlinear Empirical Modeling*: Springer Berlin Heidelberg, pp. 410, 2010.

[23] S.T. Karris, *Numerical Analysis using MATLAB and Excel*, 3rd ed. Fremont, California: Orchard Publications, pp. 8-1–8-14, 2007.

[24] N.Y. Wei, S.A. Bahari, M. Abdullah, and B. Yatim, "Regional Ionosphere Maps over Malaysia during Solar Minimum," in *Proceeding of the 2009 International Conference on Space Science and Communication,* Port Dickson, Negeri Sembilan, pp. 161-165, 2009.

[25] O.S. Bolaji, J.O. Adeniyi, S.M. Radicella, and P.H. Doherty, "Variability of Total Electron Content Over an Equatorial West African Station during Low Solar Activity," *Radio Science,* vol. 47, 2012.

[26] S.K. Leong, T.A. Musa, K.A. Abdullah, R. Othman, S. Lim, and C. Rizos, "GPS-derived Local TEC Mapping Over Peninsula Malaysia During Solar Minimum of Sunspot Cycle 24," in *Proceeding of the South East Asia Survey Congress (SEASC) 2009*, Bali, Indonesia, 2009.

[27] R.L. Harris, *Information Graphics: A Comprehensive Illustrated Reference*. New York: Oxford University Press, pp. 34, 1999.

[28] A.B.O. Jensen and C. Mitchell, "GNSS and the Ionosphere," *GPS World - INNOVATION (Signal Processing),* pp. 40-48, 2011.

[29] *The IGS Tracking Network*, https://igscb.jpl.nasa.gov/network/complete.html. 2010.

[30] J. Albert and M. Rizzo, *R by Example*: Springer New York, pp. 173-197, 2012.

[31] M.G. Marasinghe and W.J. Kennedy, *SAS for Data Analysis: Intermediate Statistical Methods*: Springer New York, pp. 222-225, 2008.

[32] C. Hagquist and M. Stenbeck, "Goodness of Fit in Regression Analysis - R^2 and G^2 Reconsidered," *Quality & Quantity,* vol. 32, pp. 229-245, 1998.

[33] A. DasGupta, A. Paul, and A. Das, "Ionospheric Total Electron Content (TEC) Studies with GPS in the Equatorial Region," *Indian Journal of Radio & Space Physics (IJRSP),* vol. 36, pp. 278-292, August 2007.